5484

NATIONAL LIBRARY
OTTAWA

BIBLIOTHÈQUE NATIONALE
OTTAWA

NAME OF AUTHOR [illegible]

TITLE OF THESIS [illegible] OF

ELECTRONS BY [illegible]

ELECTRO[illegible] [illegible] EFFECT

UNIVERSITY [illegible]

DEGREE FOR WHICH THESIS WAS PRESENTED [illegible]

YEAR THIS DEGREE GRANTED [illegible]

Permission is hereby granted to THE NATIONAL LIBRARY OF CANADA to microfilm this thesis and to lend or sell copies of the film.

The author reserves other publication rights, and neither the thesis nor extensive extracts from it may be printed or otherwise reproduced without the author's written permission.

Signed [illegible]

PERMANENT ADDRESS:

[illegible]

[illegible]

DATED Sept 4 19[illegible]

NL-91 (10-68)

[illegible]

[illegible]

[illegible]

[illegible]

[illegible]

[illegible]

[illegible]

[illegible]

by

Herbert [illegible]

[illegible] submitted [illegible]
[illegible] fulfillment
[illegible]
[illegible]

[illegible]
[illegible]
[illegible] Williams University
[illegible] April [illegible]

TABLE OF CONTENTS

ACKNOWLEDGEMENTS

The author would like to thank Professor J. M. [illegible] for suggesting the subject and for the continued aid and encouragement throughout the course of research.

He would also like to thank Mr. [illegible], who was responsible for most of the constructional work, for his excellent technical assistance with the entire experimental program.

ABSTRACT

An experimental arrangement is described in which a cylindrical electron beam, immersed in a longitudinal static magnetic field, is advancing towards a potential barrier whose height exceeds the energy of the electrons in the beam, and whose width is small relative to the length of the beam. Upon hitting the barrier, the electrons at the front of the beam are pushed over the potential barrier at the expense of the energy associated with the entire beam. In particular, in the collision of a 90 cm. long beam of 300v electrons with a square barrier of -900v height and 6 cm. width, the energy of the electrons constituting the transmitted portion of the beam was raised above 6 Kev. The beam current was 10 ma and the axial flux density of the focusing magnetic field 260 gauss.

[illegible]

[illegible] [10] [illegible]

[illegible]

[illegible]

[illegible]

[illegible]

[illegible]

[illegible]

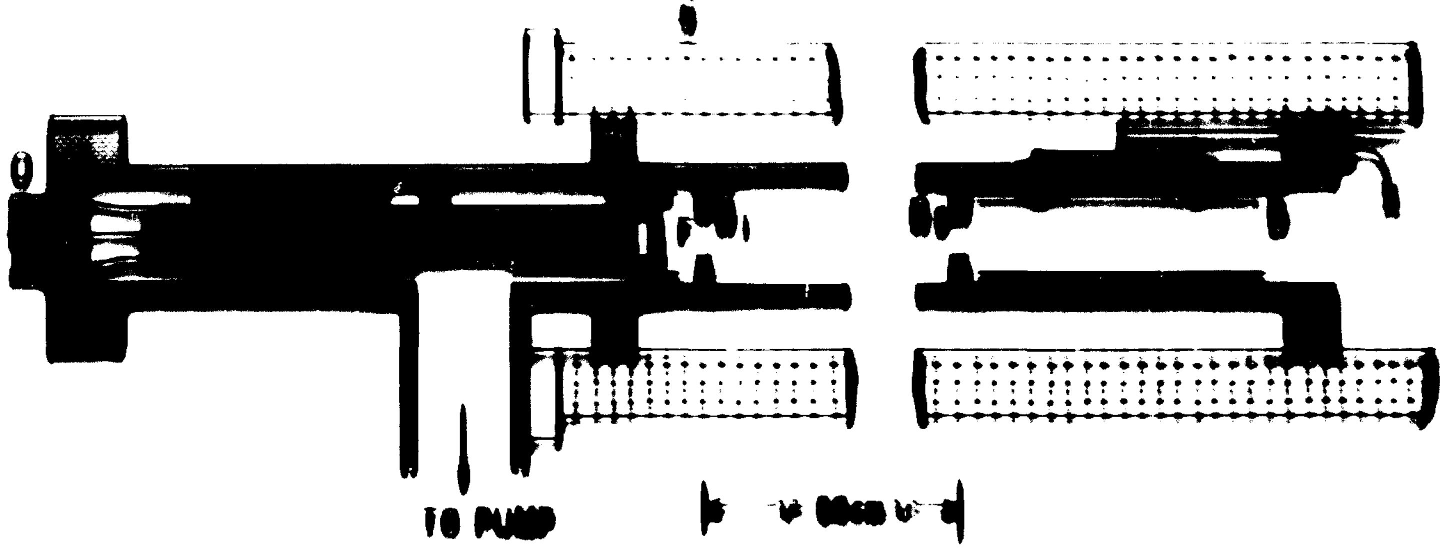

FIG 1

[illegible]

[illegible]

[illegible]

b) <u>The beam detection system</u>

Referring to Fig. [illegible], the beam detecting system comprises two cylindrical stainless electrodes of the same cross-section as the accelerator. The actual collecting cup (C), has a length of [illegible] cm and is designed such as to suppress secondary emission. Connections to the outside are provided by conductors through glass-to-metal seals, which also hold the collector rigidly in place.

The auxiliary electrode (A), of [illegible] cm length, insulated from ground, could be electrically connected to the collector. Unless used for a special purpose, it was kept at ground potential.

The entire assembly, when attached to the flange [illegible] was within the focussing magnetic field.

<u>The vacuum system</u>

The vacuum system used in this work consisted of a three-stage oil vapour diffusion pump (CVC Model [illegible] 275), backed by a rotary mechanical pump (Welch Model 1402). With a liquid nitrogen trap, the pumping process achieved during operation a vacuum of [illegible] $\times 10^{-[illegible]}$ torr. The vacuum was monitored by a Bayard-Alpert type ionization gauge

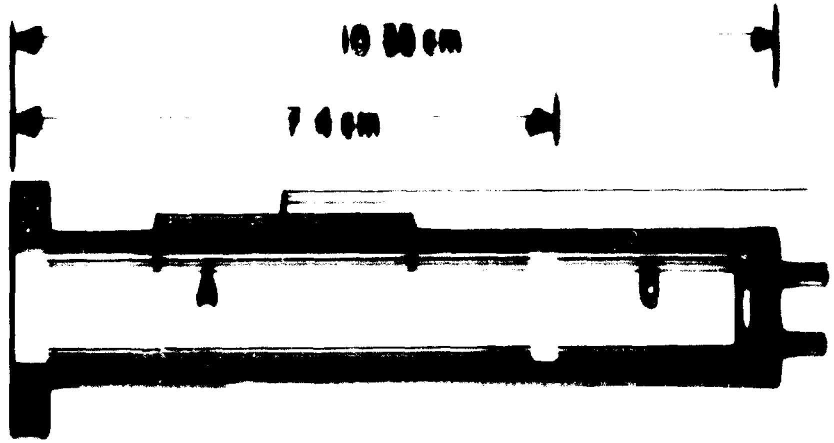

FIG 8

[illegible] [illegible] [illegible]
[illegible]
[illegible]
[illegible]
[illegible]
[illegible]

[illegible] [illegible]

[illegible]
[illegible]
[illegible]
[illegible]
[illegible]
[illegible]
[illegible]
[illegible]
[illegible]
[illegible]
[illegible]
[illegible]
[illegible]
[illegible]
[illegible]

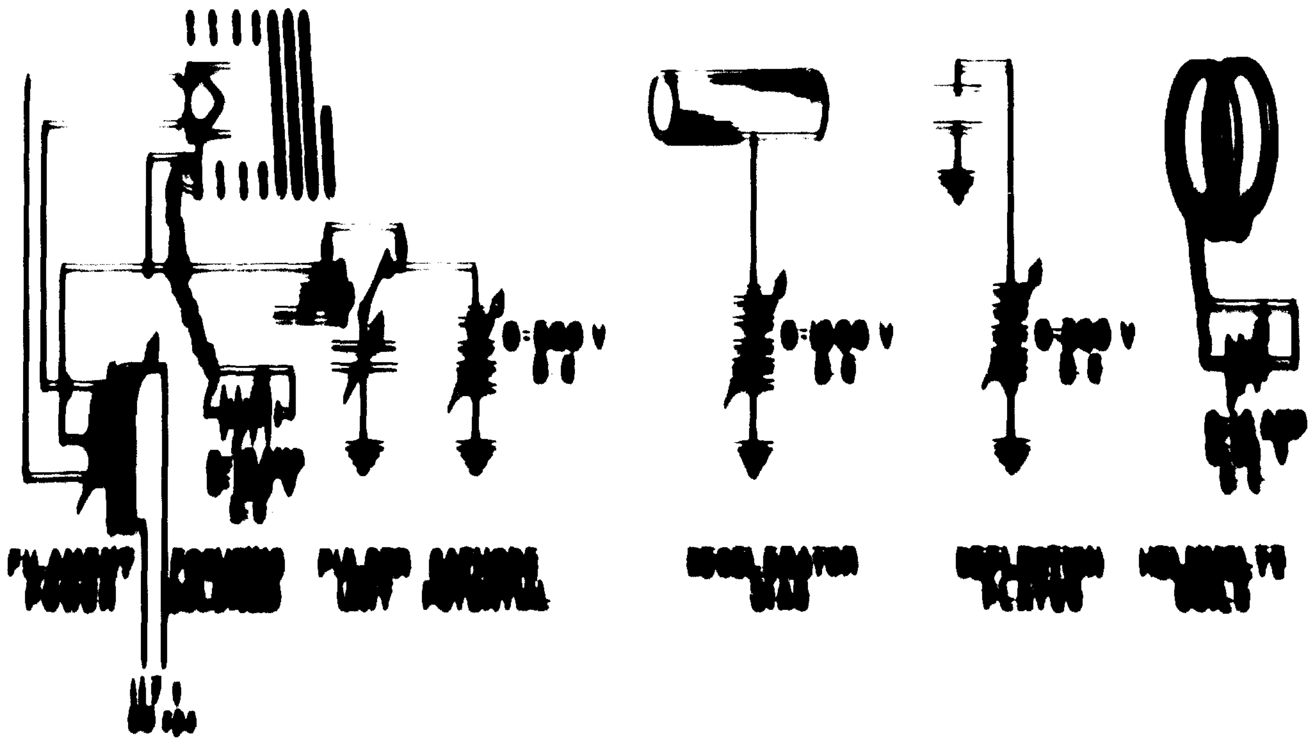

FIG 3

III Operation

The operation of the apparatus may be summed up as follows. Under the influence of the applied steady axial magnetic field, the electrons drawn from the cathode form a cylindrical stream which is coaxial with respect to the applied magnetic field. Approaching the decelerator, the axial speed of the arriving electrons is reduced to zero by the retarding electric field between tube and decelerator. This deceleration process causes an increase in space-charge density at the front of the beam, as a consequence of which the potential there drops and a potential barrier develops, against which the succeeding electrons run. Both space-charge density and barrier continue to grow until finally a space-charge limited virtual cathode is formed, the potential of which being far below that of the decelerator. As the potential barrier develops, the beam becomes decelerated, and the magnetic field associated with the beam before its deceleration collapses. During its collapse, it induces an axial electric field, that is effective only in the beam beyond the virtual cathode; along the beam in front of the virtual cathode it is balanced by an opposite electric field due to the non-uniform space-charge distribution caused by the running on of the electrons. The electric field beyond the virtual cathode, generated at the expense of the energy associated with entire beam, draws electrons from the virtual cathode and accelerates them through the decelerator towards the collector. During this discharge process, the virtual cathode disintegrates and the beam disperses under the influence of the radial interelectronic forces. The beam then re-forms, and the whole process is repeated at a frequency which depends on the operating conditions.

The apparatus may be considered to be the electronic analogue to the hydraulic ram. It is, therefore, in the following frequently referred to as the "electronic ram"; and the acceleration effect produced with this apparatus as the "ram effect".

[illegible] Preliminary Measurements

(a) Flux density of focusing magnetic field

The magnetic flux density of the long focusing solenoid was measured with a calibrated gaussmeter, as dependent on the energizing current. The following empirical relationship between flux density at its centre and current I in amperes was found:

$$B = 45\ I \quad \text{gauss}$$

A plot of the axial magnetic field within the coil vs. distance from the centre is shown in Fig. 4 for a constant current of 3.7 amperes. This was the current used for most experiments. The position of the filament of the cathode, and the position of the decelerator are also indicated on the graph.

(b) Electron current considerations

Under operating conditions the space current drawn from the cathode was, as a rule, temperature limited; hence dependent on the filament current only. For example, at an accelerating voltage of 300 volts, the space current was 5 ma when the filament current was 3.8 amps, and 10 ma, when the filament current was 4.2 amps. To increase the output to 20 ma, however,

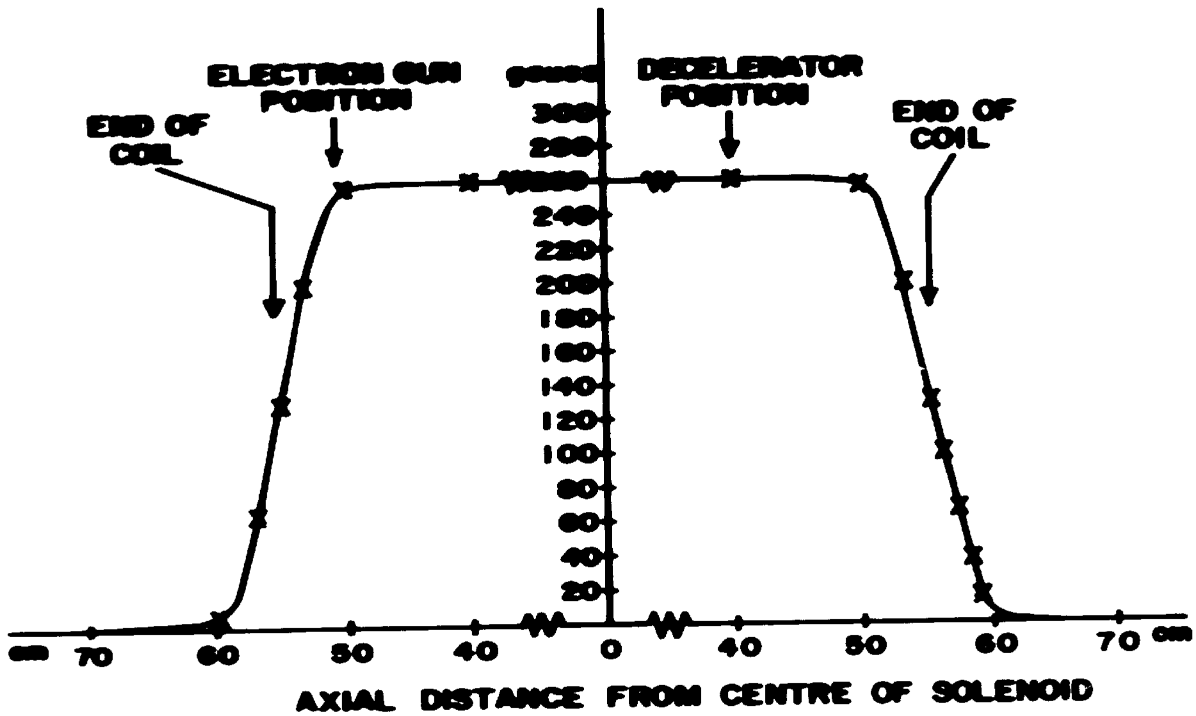

FIG. 4

Magnetic Field of Focusing Solenoid

the accelerating voltage had to be raised to 400 volts, and the filament current to 4.6 amps. To measure the current distribution to the various electrodes in the discharge device, the beam detecting equipment was joined to flange X (Fig. 1). The focusing magnetic field was adjusted to 260 gauss, the space current to 10 ma at an accelerating voltage of 300 volts. The collector, auxiliary electrode and decelerator were grounded via ammeters. Under these conditions, the current to the collector was found to be 7.5 ma, and that to the auxiliary electrode 0.3 ma. The current landing on the decelerator was negligibly small, being only 10 - 20 μamps. The baffles thus intercept about 22% of the total emission current.

(c) Output pulse with grounded decelerator

Fig. 5 shows an oscillogram of an output pulse which was obtained with a Tektronix oscilloscope, Model 543 A, when the cathode was pulsed. The pulsing capacitor of 0.0047 μfd was charged to -300 volts and intermittently connected to the cathode. The filament current was adjusted so that the peak beam current was 10 ma. The decelerator was on ground, and the focusing field 260 gauss. The collector which received the current pulse was connected to the oscilloscope via shielded cable. In the photograph, the horizontal

FIG. 5

Output Pulse Without Ram Effect

Output across 10 megohm, decelerator on ground, cathode intermittently on -300 v, beam current I_b = 10 ma, focusing field B = 260 gauss, time scale 0.5 msec/cm, sensitivity 2 v/cm, single sweep, time increases to right.

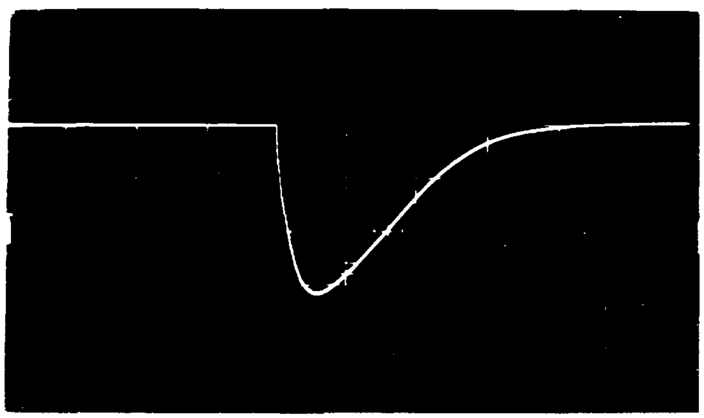

scale is 0.5 milliseconds/$_{cm}$, the vertical scale 2 volts/$_{cm}$. Time increases to the right. The total capacitance of the collector system, including the input capacitance of the oscilloscope is 21 picofarads, which is shunted by a 10 megohm resistance to ground. The pulse observed on the oscilloscope, hence depicts the voltage to which this capacitance was charged up by the electron current. The rounded top, which is due to the tail portion of the electron beam, is followed by the exponential decay of the voltage on the output capacitance. The pulse is negative, indicating an electronic current.

(d) Output pulses with negatively biased decelerator

Before proceeding to the description of the actual energy measurements, it will be shown what happens to the output pulse when the decelerator is not grounded but at a potential which is negative with respect to the cathode. The oscillogram in Fig. 6, for instance, was obtained under the same conditions as that in Fig. 5, except that the decelerator was at a potential of -600 volts with respect to ground. As distinct from the exponential decay of the output voltage, the trace of the pulse rise is invisible. Obviously the writing speed

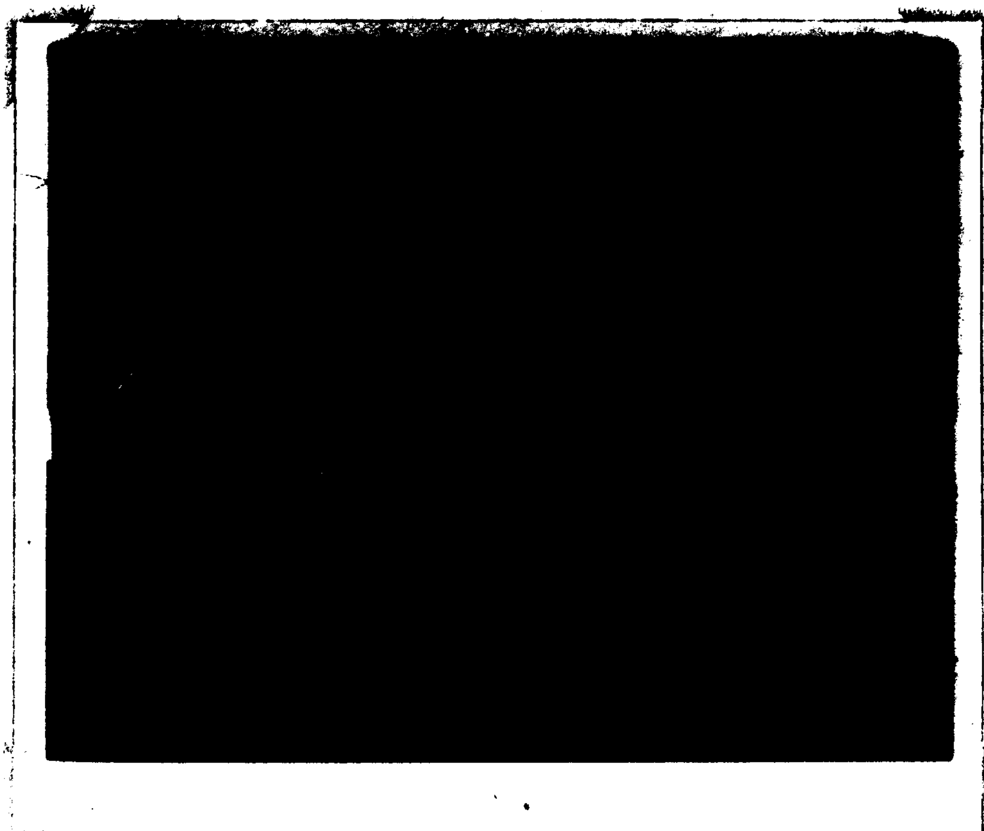

FIG. 6 (a)

Output Pulses With Ram Effect

Output across 10 megohm, decelerator on -600 v, cathode intermittently on -300 v, I_b = 10 ma, B = 260 gauss, time scale 0.5 msec/cm, sensitivity 0.5 v/cm, single sweep.

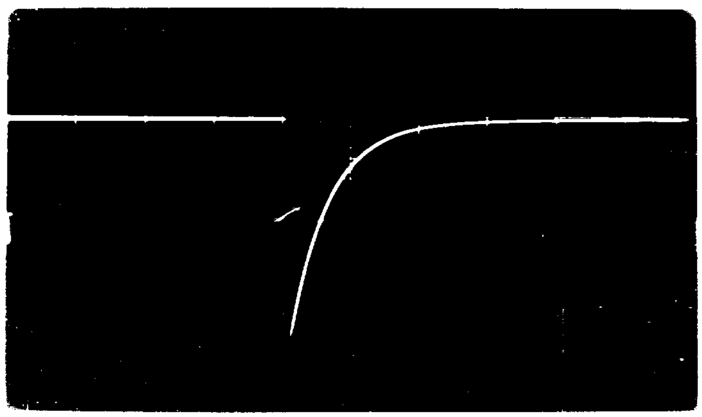

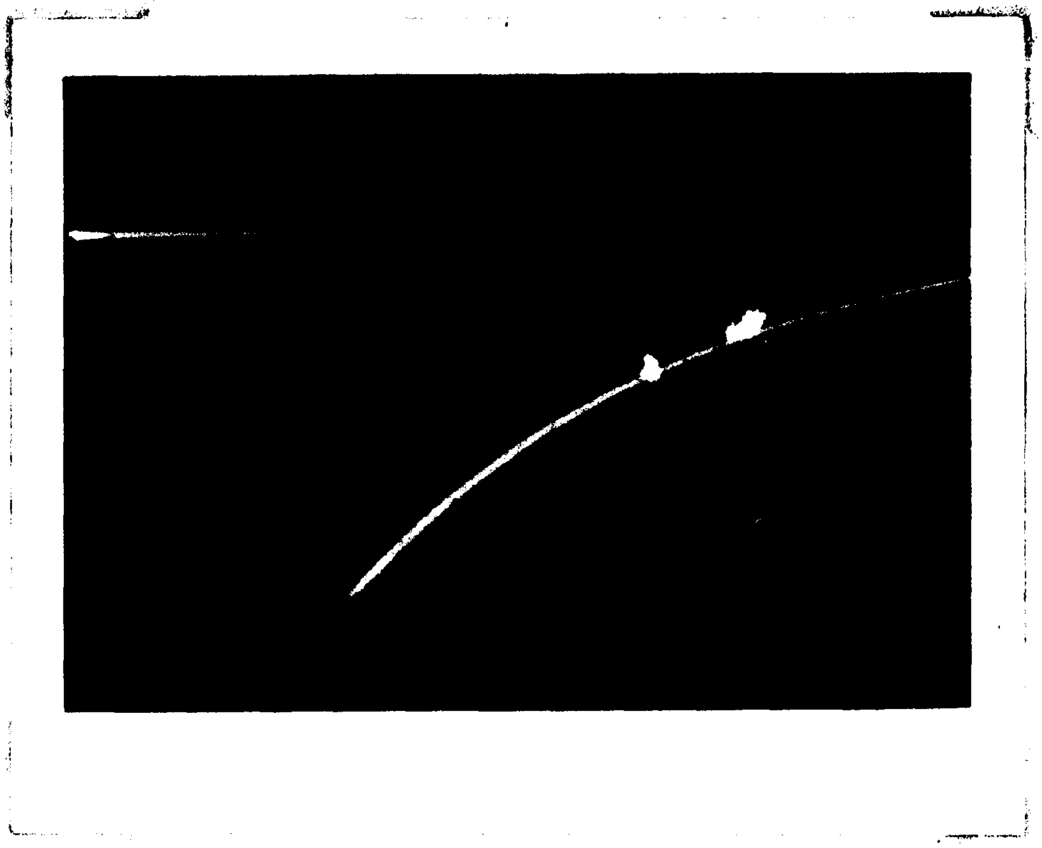

FIG. 6 (b)

Output Pulses With Ram Effect

Same conditions as 6 (a), except time scale is 0.05 msec/cm.

FIG. 6 (c)

Output Pulses With Ram Effect

Output across 1 Kohm, decelerator on -600 v, cathode continuously on -300 v, I_b = 3 ma, B = 260 gauss, time scale 0.5 msec/cm, sensitivity 0.05 v/cm, single sweep.

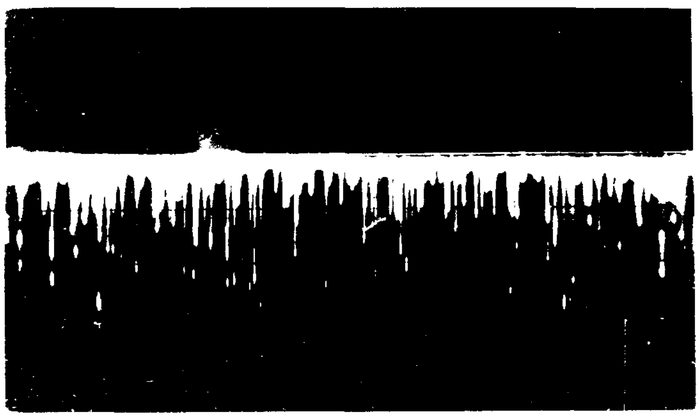

of the scope was too slow for the sudden rise. Fig. 6(b) shows a similar pulse, obtained under the same conditions, with expanded time base and higher writing intensity of the oscilloscope. Fig. 6(c) shows the output when the cathode is continuously operated. The beam current here was 3 ma, the cathode on -300 volts, the decelerator on -600 volts with respect to ground, and the focusing field was 260 gauss. The oscilloscope input in this case was shunted by a 1KΩ resistance, to reduce the time constant of the output circuit. Many small negative spikes were observed, each corresponding to an electron pulse. No satisfactory synchronization of the output pulses could be achieved to determine the "natural frequency" of the occurrence of the ram effect.

V Energy Measurements and Results

(a) Electric Deflection Method

Referring to Fig. 7, if A is the point of entry of an electron of energy eV into an electric field, its perpendicular deflection y after having travelled a distance $(L + \frac{1}{2}\ell)$ is given by the familiar formula

$$y = U\ell(L + \tfrac{1}{2}\ell)/2Vd \qquad (1)$$

where V denotes the accelerating voltage

U the deflecting voltage

ℓ the length of the deflecting plates P

L the distance between plates and collector C

y the perpendicular deflection from the axis

Accordingly, a deflecting plate system was built; it is shown schematically in Fig. 8. When connected to flange X in Fig. 1, with the beam detecting apparatus joined to flange Y as shown in Fig. 8, the following quantities of Eq. (1) are geometrically fixed at the values:

$d = 0.64$ cm

$\ell = 2.46$ cm

$(L + \frac{1}{2}\ell) = 12.33$ cm

$y = 0.37$ cm

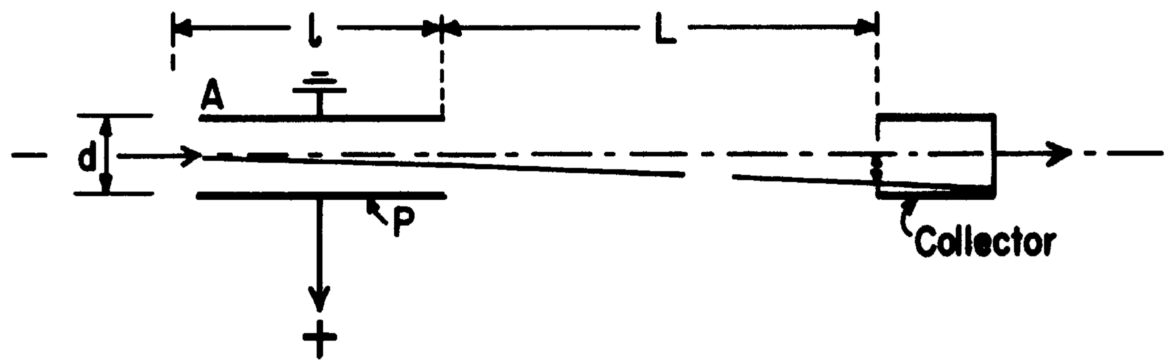

FIG. 7

Electric Deflection of an Electron Beam

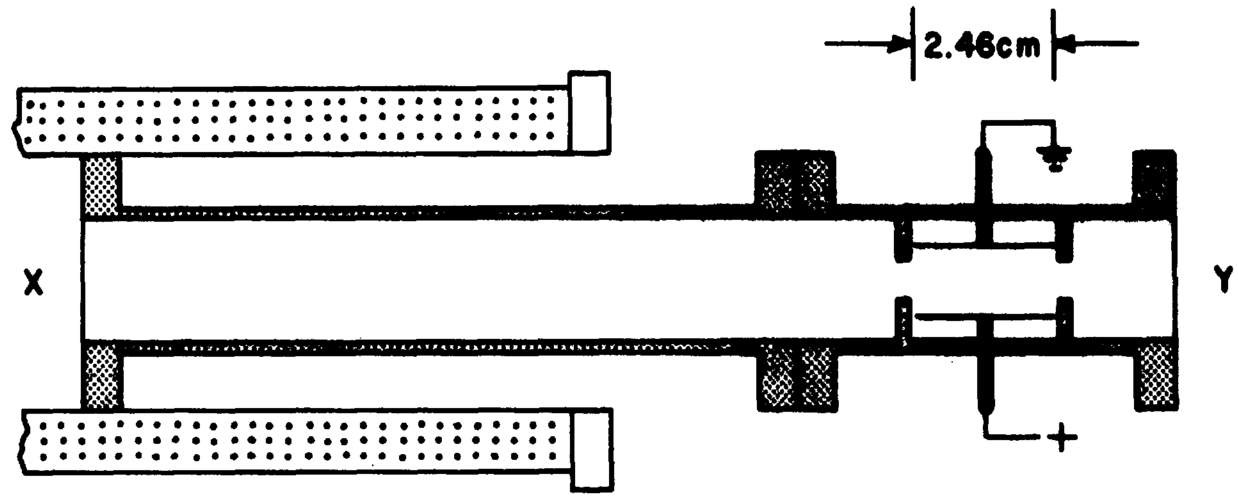

FIG.8

The Electric Deflection Plate System

Substituting these values in (1), and solving for V,

$$V = 64\ U \tag{2}$$

is obtained for the energy of electrons that just miss the edge of the collector at a deflection voltage U.

The baffles in front of and behind the deflecting plates have circular openings 0.5 cm in diameter, and the distance between the end of the decelerator and the first baffle is 19 cm.

The output current from the collector was measured with a sensitive electrometer (Keithley Model 610 A). The auxiliary electrode was held at +18 v with respect to ground by a dry battery, to suppress the emission of secondary electrons by stray primaries.

Typical results of the deflecting plates measurements are presented in Fig. 9 in form of a graph in which the collector current is plotted versus deflecting voltage for three different modes of operation. Curve (1) was obtained without ram effect, i.e., with the decelerator on ground and the cathode on -900v; curve (2) with ram effect, i.e., decelerator on -900v and the cathode intermittently on -300v relative to ground at a rate of 60 cps;

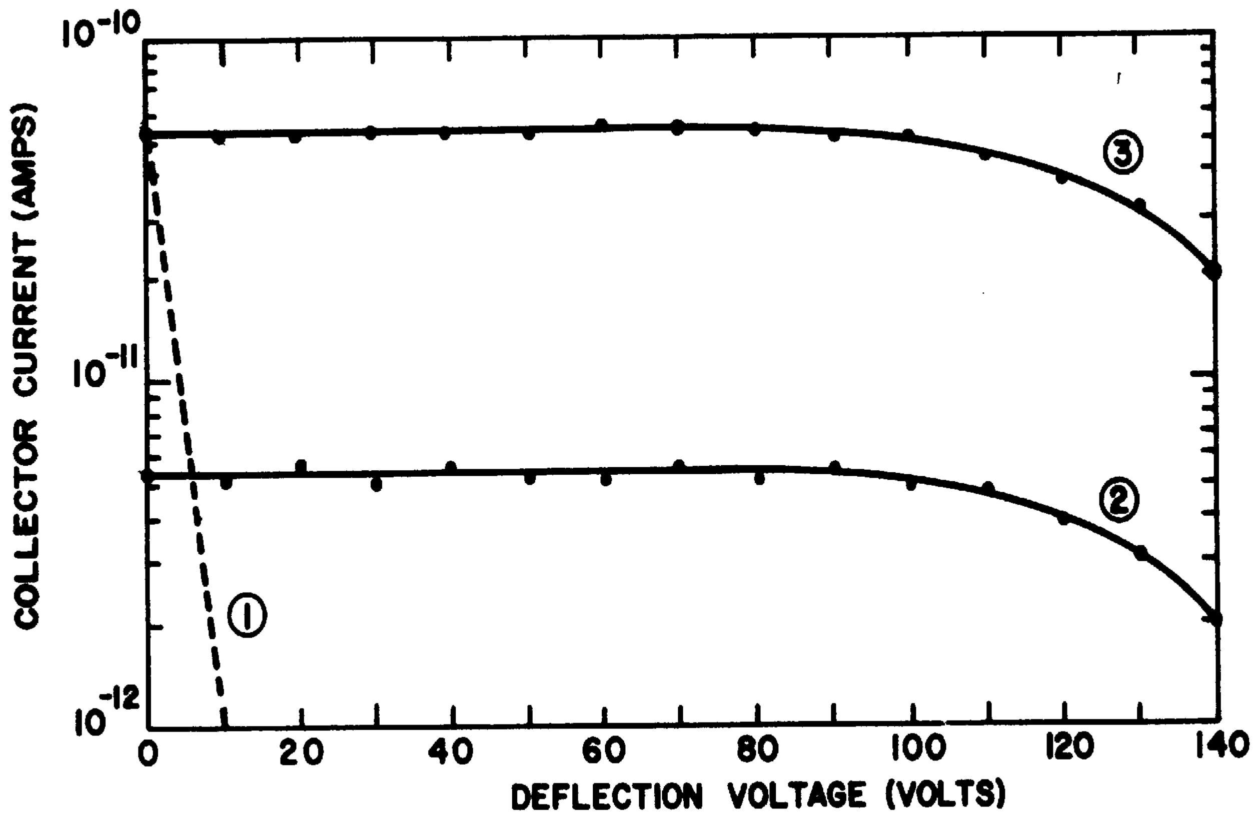

FIG. 9

Collector Current Vs. Deflecting Voltage - (1) Without ram effect
(2) With ram effect, pulsed operation
(3) With ram effect, continuous operation

curve (3) under the same conditions as curve (2), except that the cathode was not pulsed but continuously operated. The larger output in this case is due to the higher repetition rate of the ram effect. For the operation without ram effect the filament current was adjusted to give at zero deflecting voltage the same reading as for the continuous operation with ram effect. Reversing the polarity of the voltages across the deflector plates did not appreciably change the results, which indicates that the beam was well centered.

Curve (1) shows that without ram effect the output current drops rapidly as the deflecting voltage increases, being at 10 v only 1% of its initial value. Apparently the diameter of the beam was approximately equal to that of the circular hole in the baffles. The more the beam deviates from the axis the smaller the fraction of the beam that impinges on the collector.

If the cross-section of the beam were negligibly small relative to that of the aperture of the baffle, the collector current would remain constant until the voltage reaches the "cut-off" value at which the beam would just miss the collector. Theoretically, the value of the cut-off voltage for 900 v-electrons was found to be 14 v.

Table (1) gives results of deflection plate measurements under various operating conditions. Here I_b stands for beam current, E_b for beam accelerating voltage, B_f for focusing magnetic field and E_s for beam-stopping potential on the decelerator.

Table 1

Current recorded at collector as a function of deflecting voltage, under various operating conditions in units of 10^{-12} amps.

U	b	c	d	e
0	4.8	3.4	6.3	8.2
10	4.9	3.5	6.0	8.0
20	4.9	3.4	6.2	7.9
30	4.7	3.2	6.0	7.8
40	4.6	3.2	6.1	8.0
50	4.6	3.4	6.0	7.7
60	4.8	3.2	6.2	7.5
70	4.9	3.6	6.1	7.5
80	4.6	3.4	5.8	7.6
90	4.4	3.5	5.5	7.2
100	4.4	3.1	4.6	6.4
110	3.6	3.1	3.8	5.7
120	2.2	2.5	3.0	5.5
130	1.8	2.3	2.1	4.7
140	0.8	1.7	1.3	4.0

	(a)	(b)	(c)	(d)	(e)
I_b	10 ma	10 ma	5 ma	10 ma	20 ma
E_b	-300volts	-300volts	-300volts	-300volts	-400volts
B_f	260gauss	200gauss	260gauss	260gauss	260gauss
E_s	-900volts	-900volts	-900volts	-450volts	-600volts

(a) are the conditions of curve (2) Fig. 9.

(b) Magnetic Deflection Method

Suppose that, as shown in Fig. 10, an electron moving along AO meets at O the boundary of a uniform magnetic field of flux density B and direction perpendicular to axes X and Y.

Using mks units, the deflection y is given by

$$y = (e\ x^4\ B^2/8mV)^{\frac{1}{2}} \qquad (3)$$

where V is the accelerating voltage

$\frac{e}{m}$ the electronic charge to mass ratio

x the distance traversed in B

y the perpendicular deflection

B the flux density

A beta-ray spectrometer was designed and built; as schematically shown in Fig. 11.

The circular chamber was machined out of a solid piece of brass, the cylindrical cavity being 1.6 cm deep. It was sealed off by means of a

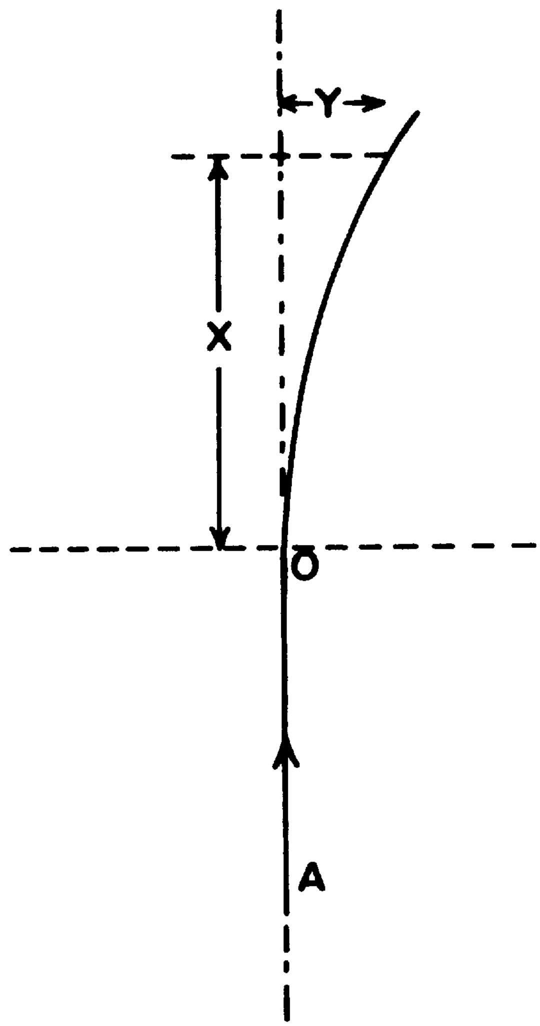

FIG. 10

Deflection by a Magnetic Field

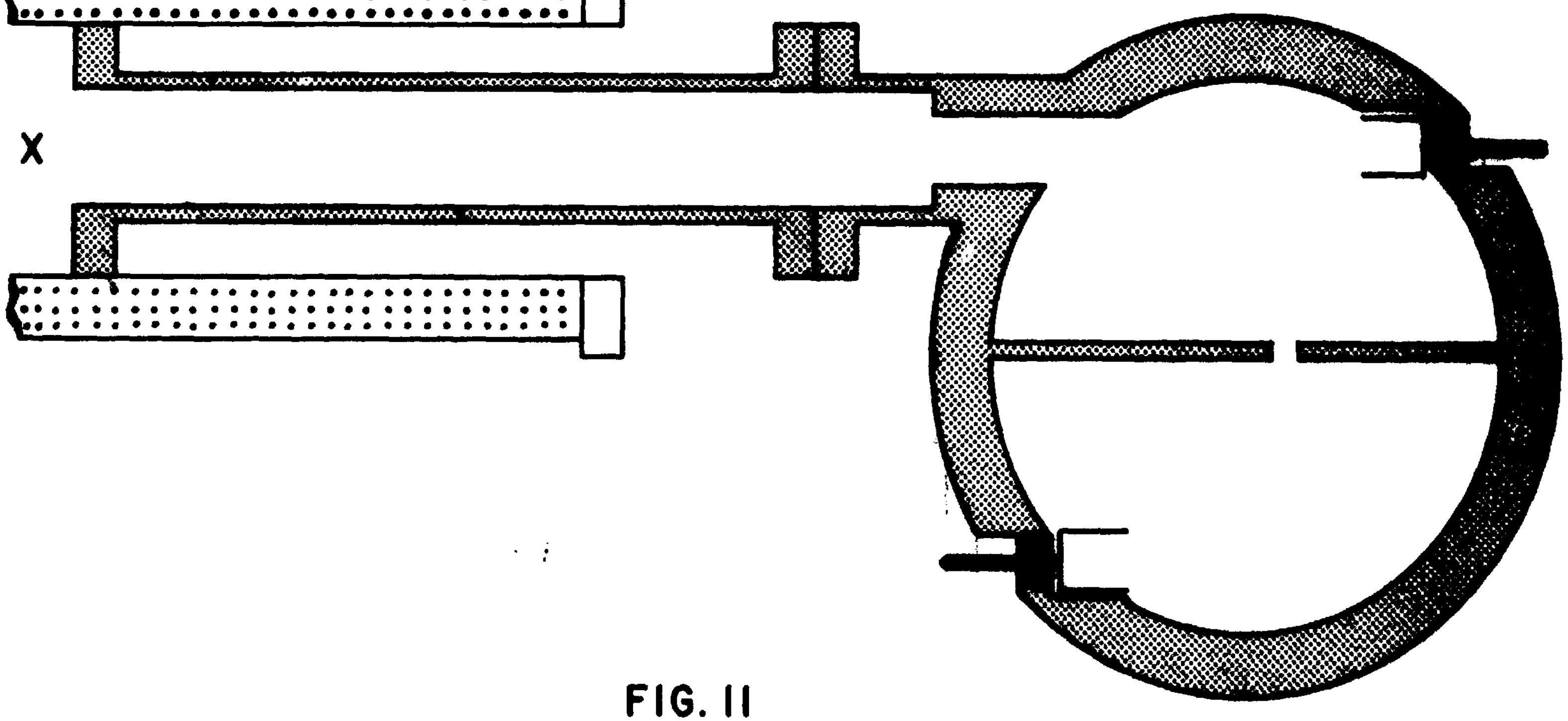

FIG. II

The Beta-Ray Spectrometer

plexiglass plate and a wire mesh screen, to shield the cavity from external fields. Two collecting electrodes and a slotted metallic partition are situated in the cavity. A set of specifically designed Helmholtz coils provided a reasonably uniform axial magnetic field. The flux density distribution is shown in Fig. 12. The Helmholtz coils could stand, for a short time a current of 14 amps; the experimentally determined relation between the coil current and the resulting average magnetic field over the electron path in gauss is

$$B = 6\ I \tag{4}$$

where I is in amperes. Originally it was intended to deflect the beam into a semicircular path through the slot to the lower collector, but the magnetic field proved to be too weak to accomplish this. Fig. 14 shows the complete experimental arrangement, with the beta-ray spectrometer attached.

Substituting the geometrically fixed values of

$x = 4 \times 10^{-2}$ m

$y = 10^{-2}$ m

and $\frac{e}{m} = 1.76 \times 10^{11}$ coul/kg

in Eq. (3), and using the relation (4), the energy V

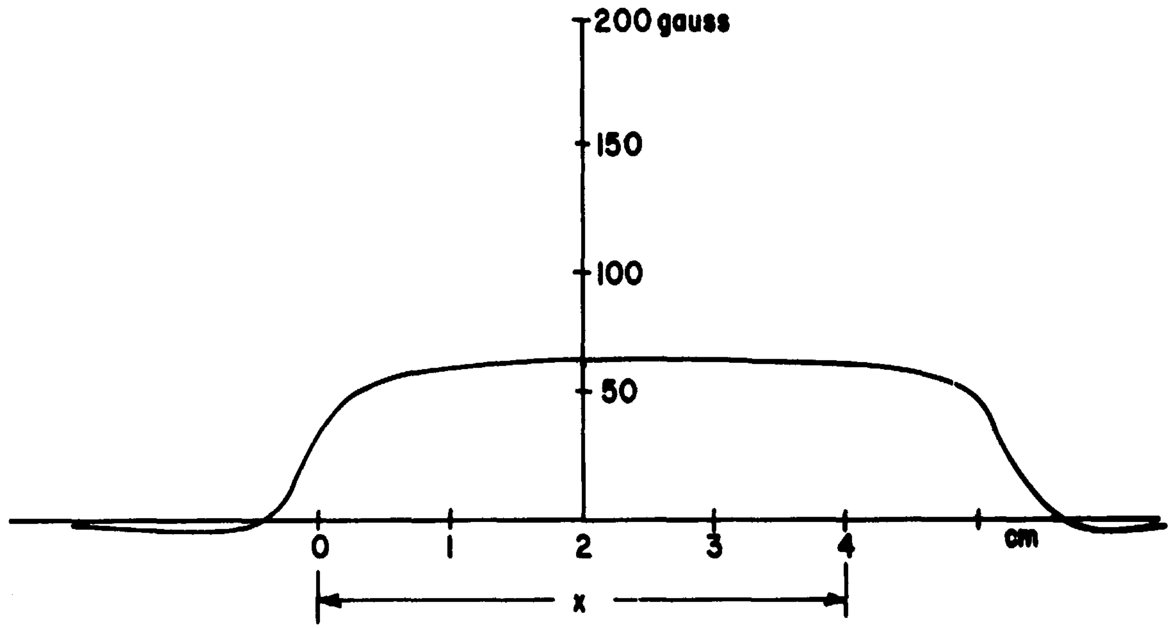

FIG. 12

Magnetic Field Distribution Over Path of Electron Beam of electrons that just miss the "in-line" collecting cup is given by

$$V = 200\ I^2 \tag{5}$$

The output current as a function of the coil current was investigated under the same operating conditions as the effect of the electric deflection. Typical results of these studies are again presented in form of a graph, in which the output current in amperes is plotted versus coil current in amperes. Curve (1) in Fig. 13 was obtained with the decelerator on ground and the cathode on -900 v relative to ground; i.e., without ram effect; Curve (2) with the decelerator on -900 v and the cathode pulsed with -300 v relative to ground; Curve (3) under the same conditions as Curve (2), except that the cathode was continuously on -300 v with respect to ground.

Consistent with the deflection plate results, varying the operating parameters did not significantly affect the results obtained. In all experiments, whenever the electron beam was deflected in front of the decelerator by means of a permanent magnet, or the focusing field turned off, or the cathode

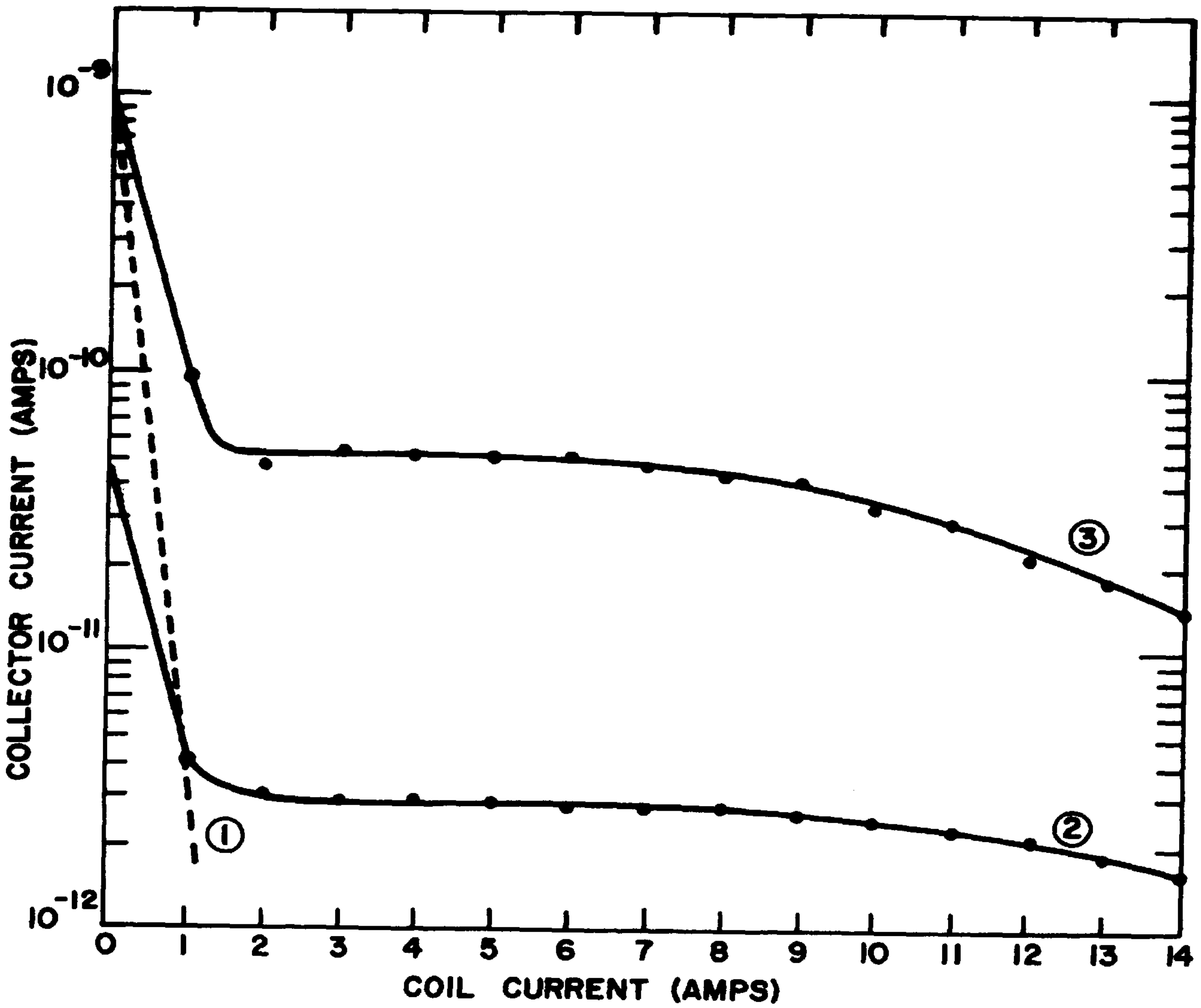

FIG. 13

Collector Current Vs. Current in Helmholtz Coils - (1) Without Ram Effect
(2) With Ram Effect, pulsed operation
(3) With Ram Effect, continuous operation.

potential removed, or the filament current turned off, the output invariably dropped to zero. This proves that the observed output was entirely due to the transmitted portion of the beam, and by no means caused by ionization or pick-up effects.

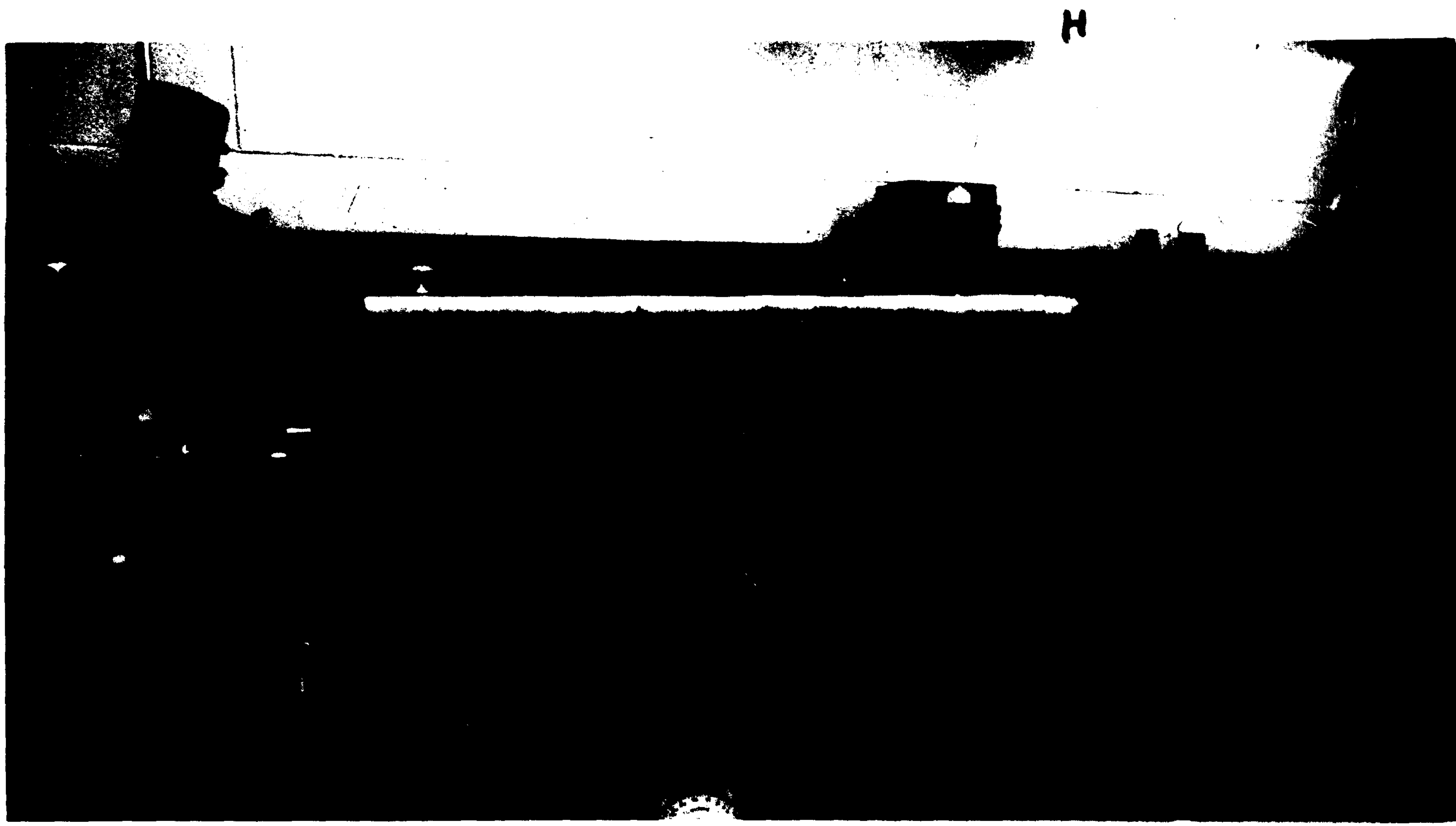

FIG. 14

The Complete Experimental Arrangement With Beta-Ray Spectrometer

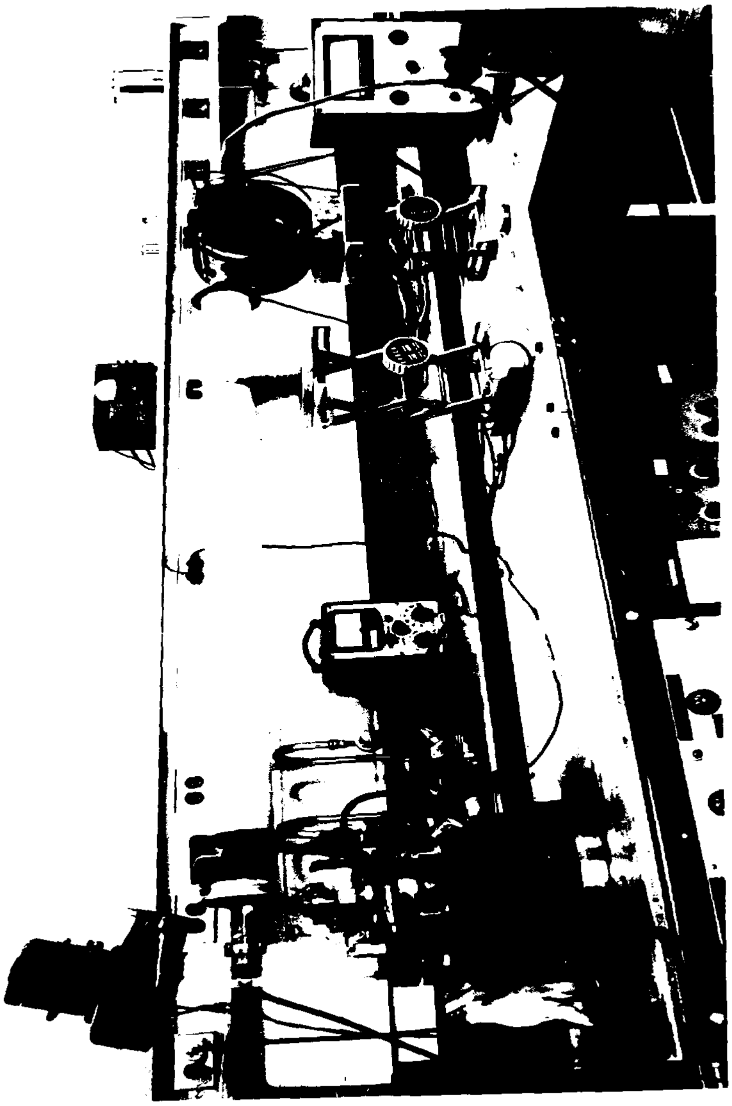

VI Discussion of Results

Comparing the shape of the output pulse in Fig. 5 with that of the output pulse in Fig. 6, one notices a drastic difference. This indicates that the discharge mechanism in the case of the negatively biased decelerator differs considerably from that with the decelerator grounded. Apart from the reduced size of the pulse in the second case due to the much smaller charge impinging on the collector, the rise of the pulse is almost instantaneous. Obviously, when the decelerator is negative with respect to the cathode, an acceleration effect occurs, which produces a burst of a small, extremely fast electronic charge.

Under continuous operation, as shown in Fig. 6(c), the ram effect takes place much more frequently, although somewhat erratically. This is not surprising in view of the inherent statistical character of the result of a collision between a beam of interacting electrons with a potential barrier. Successive beams cannot be expected to be identical in every respect. Fluctuations in the beam structure are likely to affect the entire discharge process, including deceleration, dispersion and reformation of the beam. Frequently a reformed beam may not produce an output pulse at all, e.g. when the cathode was intermittently operated, the frequency of the output pulses was always below that of the pulser. Although the time constant of the pulsing circuit was roughly 100 times larger than the transit time of the beam (0.1 usec at 300 eV), only on rare occasions was more than one output pulse per cycle of the pulser observed.

Turning now to the evaluation of the actual energy measurements of the electrons constituting these pulses, Curve (2) of Fig. 9 shows that the current, plotted versus deflection plate voltage, remains constant at 5.2×10^{-12} amps up to 100 volts. Only when the deflecting voltage exceeds 100 volts a decrease of output current sets in. Applying the relation for beam energy (3)

$$V = 64\ U,$$

one obtains for U = 100 volts an energy of 6.4 KeV for the output electrons. This, however, only represents the lowest energy in the output beam which passes through both deflection plate baffles. The current is far from being completely cut off at U = 140 volts, it actually could still be detected at U = 300 volts. Thus the electrons accelerated into the collector exhibit a spectrum of energies from 6.4 KeV upward. Curve (3) shows the same behavior, only here the average current is larger due to the more frequent occurrence of the accelerating effect. As can be seen from Curve (1), when a beam of 900 eV energy is directed through the deflecting plates, it drops sharply, and is completely cut off at U = 15 volts. The theoretical cut-off value is U = 14 volts. Referring to Table 1, variations of the operating parameters does not appreciably affect the results.

From Fig. 13, it is seen that curves (2) and (3) do not differ qualitatively. However, the presence of a soft component appears in the output, namely electrons which seem to have an energy of about 900eV. These electrons were not discovered in the deflection plate measurements because of the use of baffles. Their energy indicates that they essentially accelerated by traversing the voltage between decelerator and envelope. Consequently, they are eliminated from the output beam at a coil current of 2 amps.

The straight portion of the graph now allows an easy determination of the minimum energy of the electrons. Making use of the energy-coil current relation (5)

$$V = 200\ I^2$$

and inspecting the graphs, one finds an energy of 7.2 KeV for a coil current of 6 amps, at which value the output current begins to decrease. This energy agrees very well with the value found by the electrostatic deflection measurements.

Curve (1) again depicts the behavior of 900 eV electrons. The current drops sharply with increasing magnetic field, and is completely cut off at a coil current of 2 amps.

It is interesting to calculate the average energy of the electrons in the output pulse. With a few simplifying assumptions and the aid of the oscillograms one can estimate the average output as follows. The energy invested in the initial beam is given by

$$W_b = E_b q = E_b I_b t$$

where E_b is the accelerating voltage, q the total beam charge which is equal to the product of I_b, the beam current, and t, the transit time. The energy of the output charge Δq is

$$W_o = \tfrac{1}{2}\Delta q \bar{V}$$

where $\bar{V}$ is the average energy level of the output electrons. Assuming a 100% energy transfer from the input beam to the output beam

$$W_o = W_b$$

$$E_b q = \tfrac{1}{2}\Delta q \bar{V}$$

and

$$\bar{V} = 2E_b I_b t/\Delta q \tag{6}$$

From the oscillograms in Fig. 6(a), the output capacitance of 21 μμf is found to be charged up to 2 volts. This gives a value for Δq of 4.2×10^{-11} coulombs. The beam current I_b in this case was 10 ma, the accelerating voltage 300 volts and the transit time was 0.1 μsec. Substituting these values in Eq. (6), the average energy in eV is $\bar{V} = 15$ KeV, which in view of the assumptions is in reasonable agreement with the experimental values.

VII Conclusion

The main purpose of this work was to demonstrate that a transfer of the energy of an advancing electron beam to the electrons at the front of the beam occurs upon collision of the beam with a potential barrier whose height exceeds the energy of the electrons in the beam. To study in detail this energy transfer, further experimentation will be necessary with discharge devices which permit independent variation of the operation parameters.

VIII Reference

(1) Raudorf, W.R., Wireless Engineer, 28 (1951) 215-221.